



Effect of Acetonitrile on the Colloidal Behavior of Conventional Cationic Surfactants: A Combined Conductivity, Surface Tension, Fluorescence and FTIR Study

Ramesh Kumar Banjare¹ · Manoj Kumar Banjare^{1,2} · Sandhyarani Panda¹

Received: 6 April 2019 / Accepted: 12 October 2019 / Published online: 10 December 2019
© Springer Science+Business Media, LLC, part of Springer Nature 2019

Abstract

A comprehensive study the effect of acetonitrile (ACN) with four cationic surfactants, viz. tetradecyltrimethylammonium bromide (TTAB), cetyltrimethylammonium bromide (CTAB), cetylpyridinium chloride (CPC) and cetylpyridinium bromide (CPB) was made by using the conductivity, surface tension, fluorescence and FTIR techniques. Significant micellar, interfacial and thermodynamic properties were studied by the tensiometric and conductivity methods. The critical micelle concentration (CMC), aggregation number (N_{agg}), and Stern–Volmer constants (K_{sv}) have also been studied by the steady state fluorescence method using pyrene as probe. The fluorescence study also supports the CMC results obtained from conductivity and surface tension. FTIR was used to ascertain that the strength of intermolecular interactions such as hydrogen bonding, ion–ion pair interactions and induced dipole interactions between the surfactants and ACN depend upon the head-group of the surfactants. The interaction of surfactants with ACN is energetically favorable and occurs via direct interactions between the surfactants and ACN. The results further revealed that the strength of interactions between the surfactants and ACN follows the order: TTAB > CTAB > CPC > CPB.

Keywords Cationic surfactant · Acetonitrile · Micellization behavior · Fluorescence · FTIR spectroscopy

Electronic supplementary material The online version of this article (<https://doi.org/10.1007/s10953-019-00937-4>) contains supplementary material, which is available to authorized users.

✉ Manoj Kumar Banjare
manojbanjare7@gmail.com

✉ Sandhyarani Panda
drsandhyarani@matsuniversity.ac.in

Ramesh Kumar Banjare
rameshbanjare06@gmail.com

¹ School of Biological and Chemical Sciences, MATS University, Raipur, C.G. 492 001, India

² School of Studies in Chemistry, Pt. Ravishankar Shukla University, Raipur, C.G. 492 010, India

1 Introduction

Surfactants have attracted much attention covering a wide selection of potential applications like nano building blocks, drug delivery and associated uses as an integral part of distributed formulating systems for medicines and cosmetics [1–3]. Surface active agents (or surfactants) are amphiphilic molecules which reduce the surface tension of water [4]. Cationic surfactants possess exclusive properties, i.e. high viscoelasticity, high detergency, high solubilization, high surface wetting capability, a better tendency to lower the oil–water interfacial tension than their single chain analogues [5, 6]. These are common and versatile constitutive parts that are found in several topical cleaning agents, wetting agents, dispersants, emulsifiers, foaming agents, antiseptics, corrosion inhibitors, soaps and shampoos [6–9]. Surfactants are applied in varied merchandise due to their surface and interface activities as they cause a dramatic decrease in surface tension at low concentration [10].

The association of surface active molecules into micellar aggregates is referred to as micellization. Surfactants give rise to varied intensive properties within the solution such as ‘self-assembly’, also called micelles, and therefore the concentration at that this development happens is referred to as the critical micelle concentration (*CMC*) [11–13]. The *CMC* and form of the micelles are strongly affected by the nature of the surfactant as well as the presence of additives of the solution [14, 15]. The assorted driving forces contributing to micelle formation are van der Waals, electrical double layer, hydrophobic interaction and association forces [16–18]. The *CMC* is a crucial chemical parameter for self-assembling in surfactant solutions [19]. Solvents play a big role in the surface assimilation and micellization characteristics of surfactants [20]. Mixture of solvents and changes in the solvent properties significantly affect polarity, and carrying out adsorption and aggregation studies of surfactant provides basic data of importance [21].

Researchers have been intensively studying the influence of solvent on micellar characteristic of surfactants [22]. Micellization behavior is among the most attractive characteristics of surfactants along with their ability to provide catalytic behavior to organic reactions. Ghosh et al. [23] studied the effect of polar organic solvents, i.e. ethylene glycol and diethylene glycol on the surface adsorption and micelle formation of cationic surfactants, e.g., cetyltriethanolammonium bromide, cetyldimethylethanolammonium bromide, tetradecyldiethylethanolammonium bromide and gemini surfactants (i.e., alkanediyl- α,ω -bis(dimethylhexadecylammonium bromide) ($C_{16-s}-C_{16}$, $2Br^-$ where $s=4, 12$), butanediyl-1,4-bis(dimethyldodecylammonium bromide) ($C_{12-4}-C_{12}$, $2Br^-$) and 2-butanol-1,4-bis(dimethyldodecylammonium bromide) ($C_{12-4}(OH)-C_{12}$, $2Br^-$), by using the surface tension, conductivity and fluorescence methods. The results exhibited a rise in the *CMC* in water–organic solvents as compared to the relevant surfactants in pure water and N_{agg} modified with increasing *V/V%* of organic solvents. Kabir-ud-Din et al. [24] are systematically investigating the aggregation number (N_{agg}) of dimeric surfactants, i.e. hexamethylene-1,6-bis(tetradecyldimethylammonium bromide) in various water–organic media (i.e., 2-methoxyethanol, acetonitrile, formamide and water) and found decreased N_{agg} values in mixed media with an increase in the *V/V%* of the 2-methoxyethanol, acetonitrile and formamide. Bakshi et al. [25] studied the effect of co-solvent, i.e. ethylene glycol, glycerol, *N,N*-dimethylformamide and dimethyl sulfoxide on sodium dodecylsulfate (SDS) and cetyltrimethylammonium bromide (CTAB) using conductivity. The conductivity of SDS has also been studied in the presence of *L*-glutamic acid, 18-crown-6 ether (CR) and sucrose in aqueous solution. The results yield from the conductivity, the *CMC*, the counter ion dissociation constant (β), the standard Gibbs’ energy change of the micellization

(ΔG_m^0), and the molar equivalent conductance at infinite dilution (Λ_0) of these surfactants have been determined.

Saha et al. [26] studied the micellization of Brij-35, Brij-58, Brij-78 and Brij-98 through the formation of smaller pre-micellar aggregates and found a progressive change in the nature of the *trans*-2-[4-(dimethylamino)styryl] benzothiazole (DMASBT) molecule, which was studied using steady-state fluorescence, fluorescence anisotropy and time correlated single-photon counting measurements. The orders of occurrence of pre-micellar as well as micellar concentrations are: Brij-35 > Brij-58 > Brij-98 > Brij-78. Three different locations of DMASBT were noted for Brij-35, Brij-78 and Brij-98, whereas for Brij-58 only two locations are observed. Kartal et al. [27] studies the effect of ethanol and ethylene glycol on the micellization behavior of cetyltrimethylammonium bromide (CTAB) in aqueous solutions. The result showed at the *CMC* and the entropy increase confirmed that the micellization process is favored. Sharma et al. [28] studied the micellar behavior of conventional surfactants, i.e. cetyltrimethylammonium bromide, cetylpyridinium chloride, cetyldimethylbenzylammonium chloride, and the gemini surfactant 1,2-ethanediyl bis(dimethylhexadecylammonium bromide) 16-2-16,2Br⁻ in water and polar non-aqueous solvents (i.e., ethylene glycol, EG; dioxane, DO; dimethyl formamide, DMF and dimethyl sulfoxide, DMSO) in the temperature range from 288.15 to 318.15 K with the help of conductivity measurements. Among the studied solvents, the variation in the *CMC* is minimum in the presence of EG, whereas a maximum increase was obtained in the case of DMF.

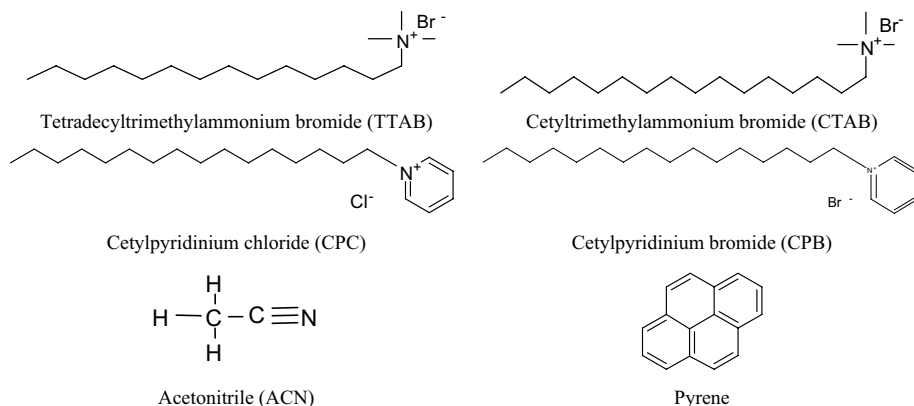
In the current study, the influence of acetonitrile (ACN) as a co-solvent on the micellization of four cationic surfactants: tetradecyltrimethylammonium bromide (TTAB), cetyltrimethylammonium bromide (CTAB), cetylpyridinium chloride (CPC) and cetylpyridinium bromide (CPB) in solution was investigated by using the conductivity, tensiometry, fluorescence and FTIR spectroscopy. The influence of the co-solvent (acetonitrile) on the *CMC* and aggregation of the conventional cationic surfactants was further characterized by calculating the degree of micellar ionization (α), degree of counter ion binding (β), and interfacial and thermodynamic parameters. The *CMC*, aggregation number (N_{agg}) and Stern–Volmer constants (K_{SV}) have been studied by the fluorescence method. The interaction behavior of ACN–surfactants was complemented using FTIR spectra. The result of this work uncovered possible applications of those solvent within the field of surfactant and colloid sciences.

The chemical structure of tetradecyltrimethylammonium bromide (TTAB), cetyltrimethylammonium bromide (CTAB), cetylpyridinium chloride (CPC) and cetylpyridinium bromide (CPB), and also acetonitrile and pyrene are shown in Scheme 1.

2 Experimental Section

2.1 Materials

Four cationic surfactants, viz. cetyltrimethylammonium bromide ($\geq 98\%$), tetradecyltrimethylammonium bromide ($\geq 98\%$), cetylpyridinium chloride ($\geq 98\%$), cetylpyridinium bromide ($\geq 98\%$), potassium bromide ($\geq 99\%$), potassium chloride ($\geq 99\%$), acetonitrile ($\geq 99.8\%$), pyrene ($\geq 98\%$) and methanol (for HPLC, $\geq 99.9\%$) were purchased from Sigma-Aldrich.



Scheme 1 Structures of tetradecyltrimethylammonium bromide (TTAB), cetyltrimethylammonium bromide (CTAB), cetylpyridinium chloride (CPC), cetylpyridinium bromide (CPB), acetonitrile and pyrene

2.2 Methods

2.2.1 Surface Tensiometer

Critical micelle concentrations (*CMC*) were determined using a surface tensiometer (Jencon, India) using the Pt-ring detachment method. The value of the surface tension was calculated as the average of the three separate measurements. The Pt-ring was cleaned with double distilled water for 8 to 10 times. The vertically hung ring was dipped into the solution to determine its surface tension.

2.2.2 Conductivity

CMC values were determined with a digital conductivity meter (Systronics direct reading Type-306). To standardize the conductivity cell constant, two totally different concentrations of potassium chloride 0.01 and 0.1 mol·L⁻¹ solutions were used. The various concentrations of cationic surfactants were gradually added into a 25 mL beaker and the conductivity values were determined at 298 K.

2.2.3 Fluorescence

The *CMC* and aggregation number of four cationic surfactants were determined using a Cary eclipse fluorescence (Agilent technology) spectrophotometer. The emission spectra of fluorescence were determined in the 350–600 nm wavelength region at the excitation wavelength of 334 nm; the slit widths for excitation and emission were 5 and 2.5 nm, respectively.

2.2.4 Fourier Transform Infrared Spectroscopy

The interaction between four conventional cationic surfactants and acetonitrile were studied by diffused reflectance–Fourier transform infrared spectroscopy (DRS-FTIR) (Model: Nicolet iS10, Thermo Fisher Scientific Instrument, Madison, USA).

3 Results and Discussion

3.1 Determination of the Critical Micelle Concentration

The most frequently used methods i.e., surface tension, conductivity and fluorescence were used for the determination of critical micelle concentrations (*CMC*) of four cationic surfactants, viz. TTAB, CTAB, CPC and CPB in the presence of acetonitrile at temperature 298 K. The resulting data of *CMC* and degree of micellar ionization (α) are given in Table 1.

3.1.1 Conductivity Measurement

The interactions of four cationic surfactants and acetonitrile (ACN) were studied using the conductivity meter. The conductance of aqueous surfactants solution on the addition of different V/V % of ACN at 298 K is presented in Figs. 1 and S1. Increases of the *CMC* seem to be caused by a stronger micelle formation as reflected in a lower α value [29]. The measured *CMC* values are reported in Table 1. For all the studied system, the

Table 1 Critical micelle concentration (*CMC*) and degree of micellar ionization (α) values of four cationic surfactants viz., tetradecyltrimethylammonium bromide (TTAB), cetyltrimethylammonium bromide (CTAB), cetylpyridinium chloride (CPC) and cetylpyridinium bromide (CPB) in water–ACN mixed medium at 298 K

ACN % (V/V)	<i>CMC</i> (mmol·L ⁻¹)			
	S.T.	Cond.	Fl.	α
TTAB				
Water	3.7(3.66) ^a ±0.018	3.8±0.030	3.6±0.019	0.26±0.031
0.5	4.1±0.020	3.9±0.026	4.0±0.032	0.34±0.035
1.0	4.5±0.021	4.2±0.011	4.6±0.033	0.38±0.032
3.0	–	11.5±0.017	10.1±0.016	0.19±0.024
CTAB				
Water	0.99(0.90) ^b ±0.012	1.0±0.034	1.0±0.011	0.26±0.041
0.5	1.6±0.011	1.6±0.015	1.5±0.012	0.50±0.038
1.0	2.5±0.018	2.6±0.025	2.5±0.010	0.56±0.046
3.0	–	2.9±0.031	3.0±0.021	0.23±0.05
CPC				
Water	0.99±0.015	1.2±0.032	1.3±0.009	0.43±0.026
0.5	1.2±0.025	1.1±0.042	1.5±0.015	0.48±0.048
1.0	1.6±0.018	1.6±0.038	2.0±0.019	0.43±0.044
3.0	–	2.2±0.022	2.3±0.021	0.93±0.035
CPB				
Water	0.9±0.022	0.9±0.021	1.2±0.010	0.40±0.021
0.5	1.1±0.024	1.0±0.019	1.5±0.021	0.52±0.034
1.0	1.5±0.016	1.3±0.018	1.8±0.012	0.58±0.031
3.0	–	2.5±0.025	3.0±0.018	0.75±0.042

S.T., surface tension; Cond., conductivity; Fl., fluorescence; α degree of micellar ionization

^aRef. [33]

^bRef. [31]

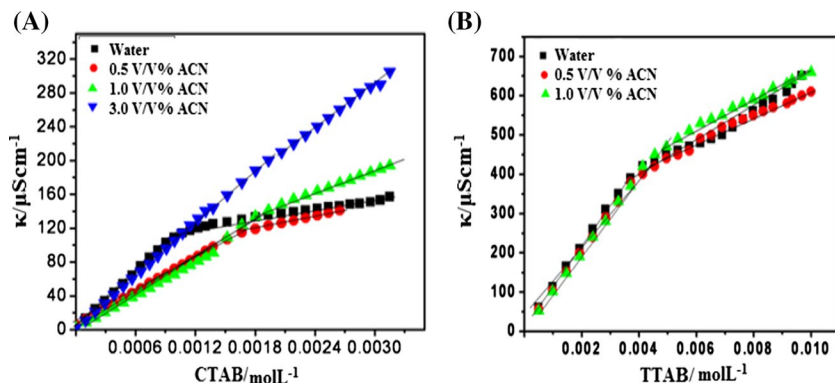


Fig. 1 **a** Specific conductivity versus CTAB concentration ($\text{mol}\cdot\text{L}^{-1}$) plots in water, 0.5, 1.0 and 3.0 V/V% of ACN at 298 K, and **b** specific conductivity versus TTAB concentration ($\text{mol}\cdot\text{L}^{-1}$) plots in water, 0.5, 1.0 V/V% of CAN at 298 K

electrical conductivity increased with increasing values of V/V% of CAN, resulting in gradual decreases of the slope [30]. The conductivity plots (Figs. 1 and S1) exhibit two linear regions in keeping with Onsager's theory: (i) pre-micelle region and (ii) post-micelle region [31].

3.1.2 Surface Tension

In the surfactant systems, the decreases the surface tension at the CMC (γ_{CMC}) of the our cationic surfactants with increases V/V% of ACN are shown in Tables 1 and 2. The plots the surface tension versus the base 10 logarithm of surfactant concentration (Figs. 2 and S2) clearly show a single break; it is thought that the CMC and γ values decrease linearly with increasing concentration for all cationic surfactant systems in the presence of ACN [31].

3.1.3 Fluorescence

Fluorescence spectra of the four cationic surfactants in solution are shown in Figs. 3, S3–S5. Pyrene is preferentially solubilized in their interior of micelles; thus it is employed to assess micellar properties. The vibronic band spectra bear vital perturbations on transferring from a non-polar to a polar setting. Because the chance of forming excitations within the sample study are often avoided by employing a low concentration of the probe, a very low concentration of the probe ($2 \text{ mmol}\cdot\text{L}^{-1}$) was used.

The fluorescence spectrum of pyrene on excitation at 334 nm shows five distinct vibronic bands at ~ 373 , 378, 383, 393 nm and 415 nm. The characteristic peaks are observed at: (i) the first vibronic bands at 373 nm and (ii) the third vibronic bands at 383 nm (pyrene may have a massive sensitivity close to any polarity modification in the micro-environment around the fluorophore). Therefore, the highest intensity ratio (I_1/I_3) of those two peaks observed in the presence and absence of the organic solvent (ACN) is employed as a tool to recognize the polarity behavior of the system, by using the I_1/I_3 ratio to calculate the CMC values, and the results are shown in Table 1 [32].

Table 2 The γ_{CMC} are the surface tension of water, surface excess concentration (Γ_{max}), surface pressure at CMC (π_{CMC}), minimum surface area per molecule (A_{min}), efficiency of absorption ($\text{p}C_{20}$), packing parameter (P) of four cationic surfactants viz., tetradecyltrimethylammonium bromide (TTAB), cetyltrimethylammonium bromide (CTAB), cetylpyridinium chloride (CPC) and cetylpyridinium bromide (CPB) in water–ACN mixed media at 298 K

ACN V/V%	γ_{CMC} (mN·m ⁻¹)	$10^6 \Gamma_{\text{max}}$ (mol·m ⁻²)	$10^{20} A_{\text{min}}$ (m ² ·mol ⁻¹)	π_{CMC} (mN·m ⁻¹)	$\text{p}C_{20}$	P
TTAB						
Water	43 ± 0.04	2.48 ± 0.02	6.68 ± 0.04	29.0 ± 0.03	2.43 ± 0.04	6.31 ± 0.02
0.5	44 ± 0.04	1.66 ± 0.02	9.99 ± 0.05	28.0 ± 0.03	2.38 ± 0.04	4.22 ± 0.02
1.0	45 ± 0.04	1.70 ± 0.02	9.76 ± 0.05	27.0 ± 0.02	2.34 ± 0.04	4.32 ± 0.04
CTAB						
Water	41 ± 0.02	2.21 ± 0.05	7.52 ± 0.03	31.0 ± 0.04	3.00 ± 0.04	5.61 ± 0.2
0.5	43 ± 0.04	1.25 ± 0.05	13.29 ± 0.04	29.0 ± 0.03	2.79 ± 0.02	3.17 ± 0.04
1.0	42.5 ± 0.06	0.79 ± 0.05	21.06 ± 0.04	29.5 ± 0.04	2.59 ± 0.04	2.00 ± 0.04
CPC						
Water	49 ± 0.04	1.17 ± 0.04	14.20 ± 0.02	23.0 ± 0.02	3.00 ± 0.02	2.97 ± 0.02
0.5	47 ± 0.04	0.85 ± 0.04	19.54 ± 0.03	25.0 ± 0.04	2.93 ± 0.02	2.16 ± 0.02
1.0	47.5 ± 0.04	1.32 ± 0.04	12.61 ± 0.06	24.5 ± 0.03	2.79 ± 0.06	3.35 ± 0.02
CPB						
Water	49 ± 0.06	0.91 ± 0.03	14.2 ± 0.03	23.0 ± 0.01	3.03 ± 0.06	2.97 ± 0.04
0.5	45 ± 0.08	0.79 ± 0.03	18.75 ± 0.03	24.0 ± 0.02	2.95 ± 0.04	2.25 ± 0.04
1.0	46 ± 0.04	1.25 ± 0.03	12.41 ± 0.05	23.2 ± 0.02	2.82 ± 0.04	3.40 ± 0.04

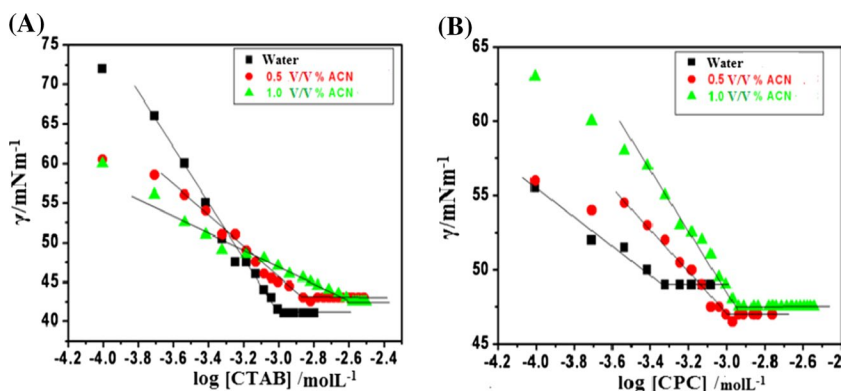
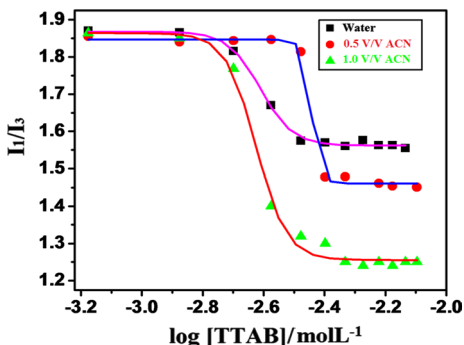


Fig. 2 Plot of surface tension against base 10 logarithm of surfactants concentration for different (V/V)% of ACN at 298 K: **a** CTAB + ACN (water, 0.5, 0.1 V/V%), and **b** CPC + ACN (water, 0.5, 0.1 V/V%)

So, to check the micelle aggregation behavior of cationic surfactants in solution, steady state fluorescence measurements were performed employing pyrene as the solvatochromic probe [32]. The fluorescence probe method was employed to verify the impact of acetonitrile on the aggregation behavior of cationic surfactants in acetonitrile solutions. This method is well-established and is usually utilized in studies related to the aggregation of cationic surfactant systems [20]. The variations in the intensity ratio (I_1/I_3) against the

Fig. 3 Plot of intensity ratio (I_1/I_3) versus logarithm of TTAB concentration ($\text{mol}\cdot\text{L}^{-1}$) in the presence of different V/V% of water–ACN solvent



concentrations of cationic surfactant (i.e., TTAB, CTAB, CPC and CPB) in water and in 0.5, 1.0 and 3.0 V/V% of ACN solutions, respectively, are shown in Figs. 3 and S3–S5. However, due to its hydrophobic nature, pyrene may be preferentially soluble and tends to interact with the hydrophobic tail part of the surfactants. The results of calculated CMC values are presented in Table 1. It is often seen that the determined CMC values are in good agreement with those obtained from both surface tension and conductivity analysis.

3.2 Effect of Acetonitrile on Cationic Surfactants

3.2.1 Effect of Acetonitrile on Interfacial Properties

The maximum surface excess concentration (Γ_{\max}) is calculated from the slope of ($d\gamma/d\log_{10}C$) using Eq. 1:

$$\Gamma_{\max} = \left(\frac{1}{2.303nRT} \right) \left(\frac{d\gamma}{d\log_{10}C} \right)_{T,p} \quad (1)$$

where Γ_{\max} is the maximum surface excess concentration of the cationic surfactants, R is the molar gas constant ($8.314 \text{ J}\cdot\text{mol}^{-1}\cdot\text{K}^{-1}$), T is the absolute temperature (Kelvin), C is the concentration of surfactant, γ is that the surface tension at a given concentration of cationic surfactant and the pre-factor constant value for cationic surfactant $n=2$ [31]. The values of Γ_{\max} were calculated using Eq. 1 and are shown in Table 2. Upon adding the different V/V% of ACN at the temperature 298 K, the Γ_{\max} value decreases with increasing V/V% of ACN. This results in the improved hydrophobic character close to the interface with the presence of ACN giving rise to the build-up of surfactants at the air–liquid interface; hence, the decrease in Γ_{\max} is observed. The order of Γ_{\max} values for binary (surfactants + ACN) systems are: TTAB > CTAB > CPC > CPB. The minimum area per molecule (A_{\min}) of cationic surfactants at the air–water interface were calculated by using Eq. 2:

$$A_{\min} = 1/\Gamma_{\max}N_A \quad (2)$$

where N_A is Avogadro's number ($6.022 \times 10^{23} \text{ mol}^{-1}$) and Γ_{\max} is the maximum surface excess concentration ($\text{mol}\cdot\text{m}^{-2}$). The calculated values of A_{\min} for the ACN are also presented in Table 2. The order obtained for the minimum area per molecule are:

TTAB < CTAB < CPC < CPB. It is evident that, since the ACN diminished the obtainable expanse for water molecules, it increasingly occupied the fraction of the interface.

The surface pressure at the CMC (π_{CMC}) was calculated as the surface tension reduction at the CMC using Eq. 3;

$$\pi_{\text{CMC}} = \gamma_0 - \gamma_{\text{CMC}} \quad (3)$$

where γ_0 and γ_{CMC} , respectively, are the surface tension of water and the surface tension at the CMC. The values of π_{CMC} at 298 K are given in Table 2 and the orders is: CTAB > TTAB > CPC > CPB. The maximum values of π_{CMC} of CTAB show highest adsorption of solvent and the lowest value of π_{CMC} of CPC.

The efficiency of adsorption was calculated from $pC_{20} = -\log_{10} C_{20}$ and are listed in Table 2. It has been determined that the pC_{20} values decrease with increase in V/V% of ACN in the binary systems. The packing parameter of surfactants in aqueous solutions with ACN was calculated by Israelachvili's model [34], during which the packing parameter (P) has been calculated using Eq. 4;

$$P = \frac{V_0}{A_{\text{min}} \cdot l_c} \quad (4)$$

where V_0 is the volume of exclusion per monomer within the aggregate, given by Tanford's formula:

$$V_0 = [27.4 + 26.9(n_c - 1)]_2 / \text{\AA}^3,$$

$$l_c = [1.54 + 1.26(n_c - 1)] / \text{\AA},$$

where l_c is the maximum chain length and n_c is the number of carbon atoms in the hydrocarbon chain and was taken as being 16, 14, 16 and 16 for the CTAB, TTAB, CPC and CPB, respectively. The values of the packing parameter (P) are listed in Table 2.

Sugihara et al. [35] have considered that a thermodynamic quantity for the analysis of synergism in micellar resolution and also the Gibbs energy of the air/water interface ($\Delta G_{\text{min}}^{(s)}$) is to be calculated using Eq. 5:

$$\Delta G_{\text{min}}^{(s)} = A_{\text{min}} \cdot \gamma_{\text{CMC}} \cdot N_A \quad (5)$$

where γ_{CMC} is the surface tension of the cationic surfactants system at equilibrium. The $\Delta G_{\text{min}}^{(s)}$ values are lowest when a more thermodynamically stable surface is formed and evaluation of the system is synergistic [30]. The calculated data are show in Table 3. It may be seen that a minimal (most negative), not maximal value, of ΔG_{min}^0 was obtained in the case of CPC in 0.5% ACN solution. The highest value was obtained for both CPC and CPB in pure water.

3.2.2 Effect of Acetonitrile on the Thermodynamic Parameters

Adsorption and micellization processes of the surfactant molecules are considered as phase transformations, either from separate molecules within the solution into absorbable molecules at the interface (adsorption), or into the well-aggregated molecules in the form of

Table 3 Thermodynamic parameters, i.e., counter ion binding (β), Gibbs energy of micellization (ΔG_M^o), the standard Gibbs energy of adsorption (ΔG_{ads}^o), the Gibbs energy of transfer (ΔG_{trans}^o), the Gibbs energy at air–water interface (ΔG_{min}^o), and the Gibbs energy of micellization per alkyl tail (ΔG_{tail}^o) for four cationic surfactants viz., tetradecyltrimethylammonium bromide (TTAB), cetyltrimethylammonium bromide (CTAB), cetylpyridinium chloride (CPC) and cetylpyridinium bromide (CPB) in water–ACN mixed media at 298 K

ACN % (V/V)	β	ΔG_M^o (kJ·mol ⁻¹)	ΔG_{ads}^o (kJ·mol ⁻¹)	ΔG_{trans}^o (kJ·mol ⁻¹)	ΔG_{tail}^o (kJ·mol ⁻¹)	ΔG_{min}^o (kJ·mol ⁻¹)
TTAB						
Water	0.74 ± 0.50	-11.5 ± 0.034	-23.2 ± 0.046	-	-5.79 ± 0.036	17.3 ± 0.5
0.5	0.66 ± 0.54	-10.8 ± 0.032	-27.7 ± 0.040	0.73 ± 0.4	-5.43 ± 0.042	26.4 ± 0.5
1.0	0.62 ± 0.53	-10.4 ± 0.040	-26.3 ± 0.050	1.16 ± 0.6	-5.22 ± 0.044	26.4 ± 0.4
3.0	0.81 ± 0.48	-7.09 ± 0.044	-	4.50 ± 0.4	-3.55 ± 0.048	-
CTAB						
Water	0.74 ± 0.54	-17.3 ± 0.044	-31.0 ± 0.034	-	-8.69 ± 0.046	18.5 ± 0.6
0.5	0.66 ± 0.46	-13.2 ± 0.046	-36.4 ± 0.038	4.12 ± 0.2	-6.63 ± 0.052	34.4 ± 0.4
1.0	0.81 ± 0.50	-10.9 ± 0.040	-48.7 ± 0.044	6.44 ± 0.4	-5.47 ± 0.028	53.9 ± 0.6
3.0	0.77 ± 0.52	-13.06 ± 0.054	-	4.32 ± 0.4	-6.53 ± 0.036	-
CPC						
Water	0.56 ± 0.56	-6.03 ± 0.028	-25.7 ± 0.054	-	-3.02 ± 0.042	42.0 ± 0.4
0.5	0.52 ± 0.58	-14.8 ± 0.022	-44.3 ± 0.060	8.83 ± 0.6	-7.43 ± 0.028	55.3 ± 0.6
1.0	0.57 ± 0.48	-13.9 ± 0.044	-32.5 ± 0.048	7.87 ± 0.4	-6.95 ± 0.054	36.1 ± 0.2
3.0	0.07 ± 0.50	-8.6 ± 0.048	-	2.61 ± 0.6	-4.32 ± 0.044	-
CPB						
Water	0.60 ± 0.52	-6.0 ± 0.046	-25.70 ± 0.046	-	-3.02 ± 0.048	42.00 ± 0.4
0.5	0.48 ± 0.54	-20.1 ± 0.042	-50.46 ± 0.052	14.05 ± 0.8	-10.04 ± 0.042	55.08 ± 0.6
1.0	0.42 ± 0.48	-19.8 ± 0.038	-38.42 ± 0.040	13.83 ± 0.4	-9.93 ± 0.034	33.43 ± 0.4
3.0	0.25 ± 0.50	-15.4 ± 0.040	-	9.38 ± 0.4	-7.70 ± 0.052	-

micelles; this phenomena is known as micellization. The degree of micellar ionization was calculated from the slopes of the two linear curves of conductivity as described by Eq. 6:

$$\alpha = S_1/S_2 \quad (6)$$

where S_1 and S_2 are the pre- and post-micellar slopes of the surfactant. In conductivity plots Figs. 1 and S1, this phenomenon appears as a decrease in slope after the *CMC* point. The ratio of the post-*CMC* slope to the pre-*CMC* slope is defined as the micellar ionization degree (α) [30]. The calculated values for the degree of ionization (α) and the counter ion binding (β) of the micelles are summarized in Table 1 and 3. Experimental data support the suggestion that the nature of the counter ion has a vital influence on the micellization of surfactants.

The standard Gibbs energy of micellization (ΔG_M^o) is,

$$\Delta G_M^o = (2-\alpha)RT \ln X_{CMC} \quad (7)$$

$$X_{CMC} = C_{CMC}/55.4 \quad (8)$$

where X_{CMC} is the CMC in mole fraction, C_{CMC} is in $\text{mol}\cdot\text{L}^{-1}$ and 55.4 comes from 1 L of water at 298 K and α is that the micellar ionization fraction whose calculated values are reported in Table 1. The addition of ACN to transfer the hydrophobic tail from the bulk phase to the micellar region is more favorable. Hence, the ΔG_M^0 value decreases for CTAB and TTAB, but for CPC and CPB the ΔG_M^0 value increase as the result of the presence in the pyridinium cluster of delocalized π -electron. This shows that the micellization process becomes spontaneous with decreasing V/V% of ACN. The ΔG_M^0 value gradually decreases with higher volume percentage of the solvent. The calculated ΔG_M^0 values are reported in Table 3 and the spontaneity of micellization order is: CTAB > TTAB > CPC > CPB.

The standard Gibbs energy of adsorption (ΔG_{ads}^0) has been calculated using Eq. 9:

$$\Delta G_{ads}^0 = \Delta G_M^0 - \pi_{CMC}/\Gamma_{max} \quad (9)$$

Surfactants are hydrophobic by nature and easily aggregate with ACN as solvent to form a micelle. The ΔG_{ads}^0 value is larger than of ΔG_M^0 for all systems. The maximum value of ΔG_{ads}^0 was determined for the TTAB + 1.0 V/V% of ACN combination, and the minimum value (most negative), is observed in the case of CPB in 0.5% ACN. The V/V% of ACN increase corresponds to increasing of the ΔG_{ads}^0 values, and these values support micellization is dominant over adsorption on the solution.

The Gibbs energy of micellization per alkyl tail ($\Delta G_{M,tail}^0$) was calculate from Eq. 10,

$$\Delta G_{M,tail}^0 = \Delta G_M^0/2 \quad (10)$$

The $\Delta G_{M,tail}^0$ values of the cationic surfactants are listed in Table 3, which shows that the surfactant tail is removed from contact with solvent mixtures and transferred to the hydrophobic core of the micelle. So, the effect of solvent on the micellization process was calculated through the Gibbs energy of transfer (ΔG_{trans}^0) which can be written as;

$$\Delta G_{trans}^0 = \Delta G_M^0(\text{water - organic solvent mixed medaa}) - \Delta G_M^0(\text{in putr water}) \quad (11)$$

The addition of various V/V% of organic solvents makes the bulk phase a better solvent for the surfactant molecules and also the hydrophobic tail transfer from the bulk phase into micelles becomes less favorable. As a consequence, ΔG_{trans}^0 decreases with increase in the CMC . The positive values of ΔG_{trans}^0 may be explained on the premise of a reduction within the solvophobic interactions caused by improved solvation. The causes a rise in the solubility of the hydrocarbon tails in the presence of ACN and, consequently, in a rise as seen in the result shown in Table 3. The ΔG_{trans}^0 value gradually decreases with increasing V/V% of ACN in the mixture. This results from the advantageous interactions of the hydrocarbon part of a surfactant with the ACN solvent and the cationic head with water that decrease the flexibility of a surfactant to associate.

3.3 Aggregation Number and Microenvironment Study

The aggregation number of cationic surfactants may be determined from the Turro–Yekta methodology [36]:

$$\ln\left(\frac{I_0}{I_Q}\right) = \frac{N_{agg}[Q]}{[S] - CMC} \quad (12)$$

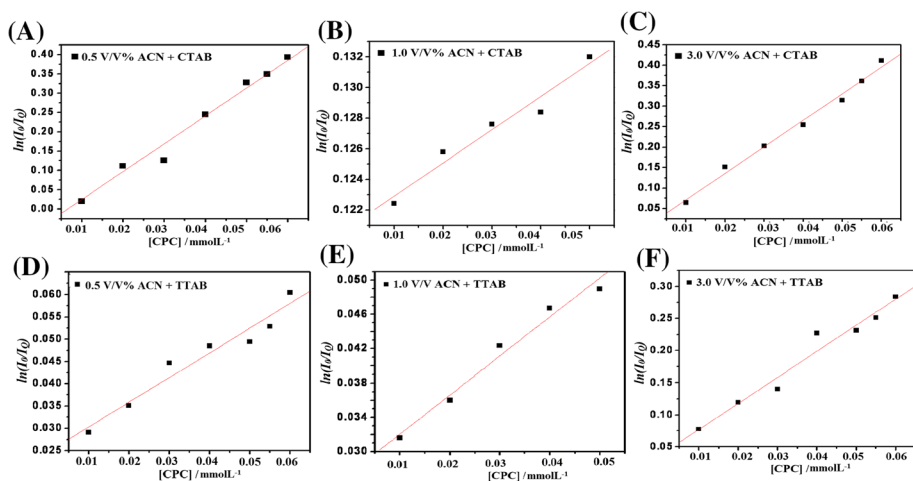


Fig. 4 Fluorescence quenching by CPC in $120 \text{ mmol}\cdot\text{L}^{-1}$ aqueous cationic surfactants in the presence of different V/V% of CAN: **a** [CTAB]+0.5 V/V% CAN, **b** [CTAB]+1.0 V/V% ACN, **c** [CTAB]+3.0 V/V% ACN, **d** [TTAB]+0.5 V/V% ACN, **e** [TTAB]+1.0 V/V% ACN and **f** [TTAB]+3.0 V/V% ACN

Table 4 Critical micelle concentration (CMC), aggregation number (N_{agg}), and Stern–Volmer constants (K_{sv}) of tetradecyltrimethylammonium bromide (TTAB) and cetyltrimethylammonium bromide (CTAB) in water, 0.5, 1.0 and 3.0 V/V % of acetonitrile

ACN % (V/V)	CTAB			TTAB		
	CMC ($\text{mmol}\cdot\text{L}^{-1}$)	N_{agg}	K_{sv}	CMC ($\text{mmol}\cdot\text{L}^{-1}$)	N_{agg}	K_{sv}
Water	1.0 ± 0.011	59 ± 0.5	0.60 ± 0.02	3.6 ± 0.019	40 ± 0.4	0.88 ± 0.04
0.5	1.5 ± 0.012	38 ± 0.5	0.40 ± 0.04	4.0 ± 0.032	25 ± 0.4	0.55 ± 0.06
1.0	2.5 ± 0.010	13 ± 0.5	0.21 ± 0.02	4.6 ± 0.033	21 ± 0.4	0.45 ± 0.04
3.0	3.0 ± 0.021	9 ± 0.5	0.11 ± 0.06	10.1 ± 0.016	15 ± 0.4	0.06 ± 0.02

Here I_0 and I_Q are the fluorescence intensities of the surfactant solution with pyrene (at 373 nm) in the absence and presence of quencher (cetylpyridinium chloride). $[Q]$ and $[S]$ denote the concentrations of quencher and concentration of cationic surfactant, respectively. Figure 4 shows the plots of $\ln(I_0/I_Q)$ against concentration of $[CPC]$ ($\text{mmol}\cdot\text{L}^{-1}$) by using the slope to estimate the aggregation number (N_{agg}) using Eq. 12 of the cationic surfactant in the organic solvent media. It was observed that N_{agg} values of both cationic surfactants (i.e., CTAB and TTAB) decrease with increasing V/V% of the organic solvent in the mixed media and that results in lower numbers of molecules in the micelles (Table 4). For each type of surfactant molecule, the rate of decrease is nearly the same in both aqueous and organic media. In the present study, the microenvironment of self-assembly, studied by fluorescence, were carried out using pyrene as a probe and, as a result, the pyrene is bound preferentially to the hydrophobic region of the self-assemblies [37].

The change in micropolarity of pyrene in ACN solutions is greater than that with solutions of different surfactants. The extent of micropolarity in the case of TTAB cationic surfactant micelle is higher, signifying more solubilization in aqua-organic media because

of attractive interactions. The lesser solubilization of the C_{16} head group of CTAB, owing to electrostatic repulsion, results in the lower value of micro-polarity. The aggregation number decreases with increasing solvent polarity.

3.4 Fourier-Transform Infrared Spectroscopy

FTIR is that the most advantageous method for classifying organic or inorganic chemicals and detection of intermolecular interactions in surfactants molecules [38], and to deduce insightful information about the molecular structure and molecular interactions prevailing within the chemical system. It is employed to analyzed quantitative mixtures of compounds and analysis of solids, liquids and gases [39]. In the present study, FT-IR spectra of the four cationic surfactants, cetyltrimethylammonium bromide (CTAB), tetradecyltrimethylammonium bromide (TTAB), cetylpyridine bromide (CPB) and cetylpyridine bromide (CPC) in aqueous acetonitrile have been measured using a Nicolet iS10 (Thermo Fisher) FT-IR spectrophotometer. These FT-IR spectra for CTAB, TTAB, CPC and CPB and concentrations at the CMC are shown in Figs. 5, 6, 7 and 8. To provide more insight into the interaction between the cationic surfactants and solvent, the system was characterized by FT-IR. The stretching frequency of the pure cationic surfactant molecules and their mixtures with acetonitrile are listed in Table 5, which show that mixtures with acetonitrile shift the stretching frequency of IR spectra.

The absorption peaks of CTAB are shown in Fig. 5; symmetric and asymmetric stretching CH_2 vibrations of alkyl chains are found at 2850 cm^{-1} and 2917 cm^{-1} but are shifted to 2855 cm^{-1} and 2920 cm^{-1} . The symmetric and asymmetric stretching C–H scissoring vibration of the CH_3-N^+ moiety at 1480 cm^{-1} is shifted to 1469 cm^{-1} , the C– N^+ stretching bands at 961.3 cm^{-1} is shifted to 1097 cm^{-1} in the [CTAB]–acetonitrile complex. The absorption peak of TTAB is shown in (Fig. 6), the alkyl C–H stretch at 2915.72 cm^{-1} is shifted to 2917.75 cm^{-1} , the *trans* = C–H out-of-plane bending at 910.99 cm^{-1} is shifted to 913.29 cm^{-1} , the *cis* = C–H out-of-plane bending 718.62 cm^{-1} is shifted to 725.55 cm^{-1} .

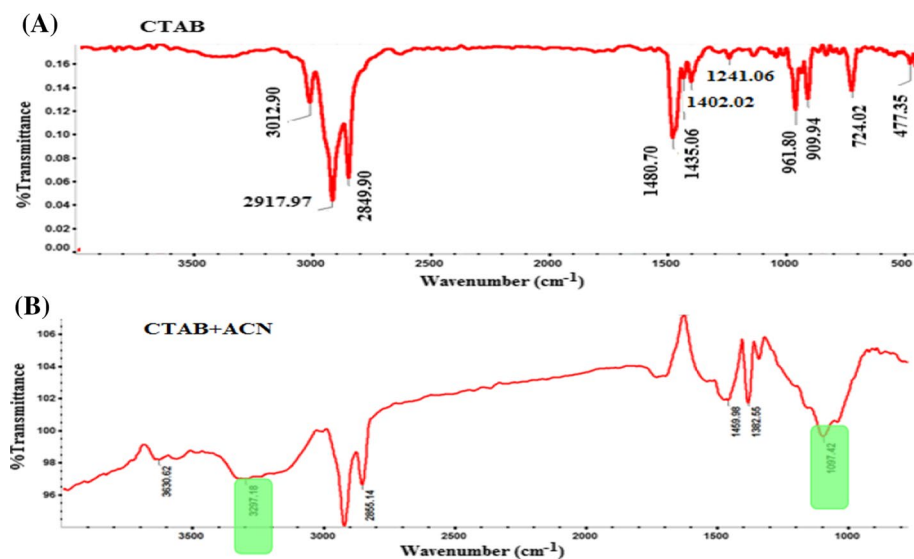


Fig. 5 DRS-FTIR spectra of a pure CTAB and b CTAB–ACN

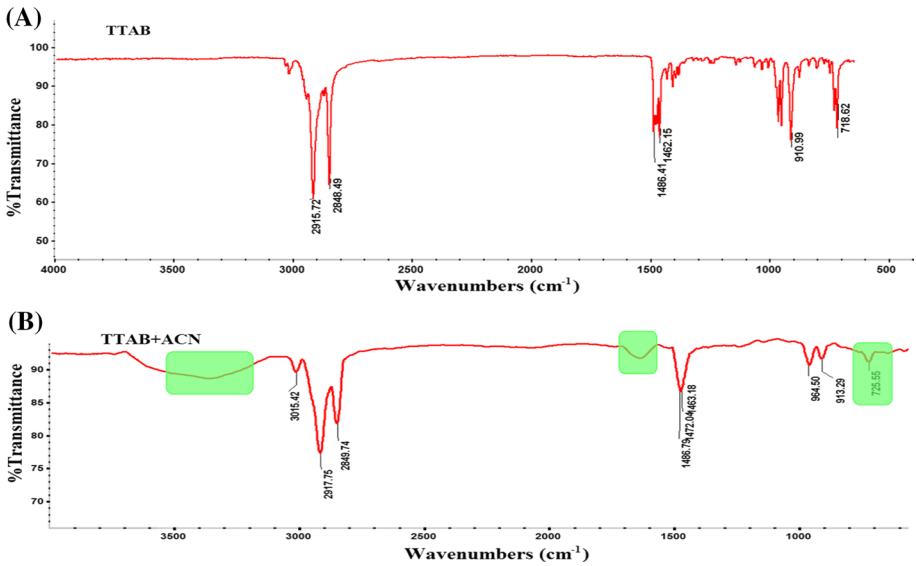


Fig. 6 DRS-FTIR spectra of **a** pure TTAB and **b** TTAB-ACN

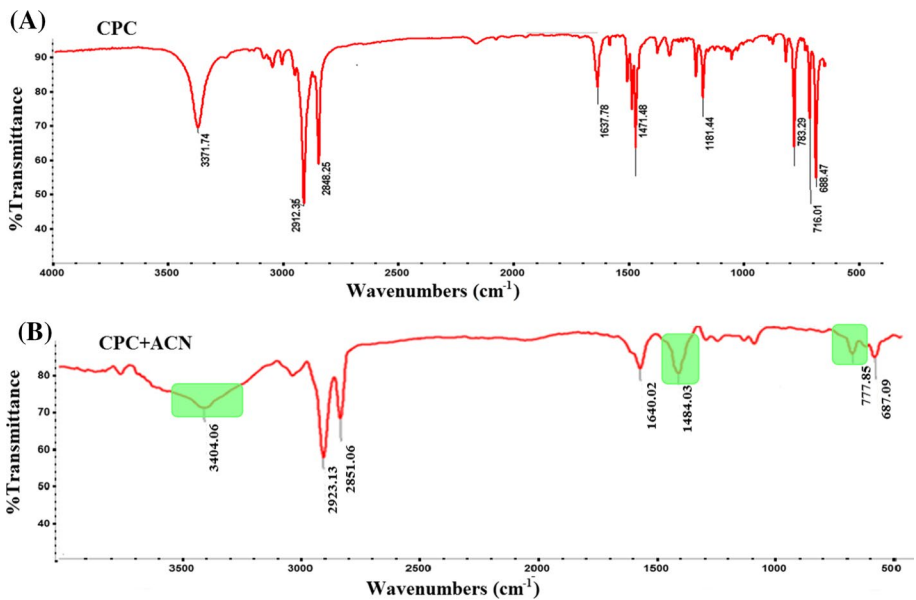


Fig. 7 DRS-FTIR spectra of **a** pure CPC and **b** CPC-ACN

The absorption peak of CPC are shown in (Fig. 7), the O-H stretching at 3371.74 cm^{-1} is shifted to 3404.06 cm^{-1} , the asymmetric CH_2 , symmetric CH_3 , CH_2 stretching vibration at 2912.35 cm^{-1} is shifted to 2923.13 cm^{-1} , the alkyl C-H stretch at 2848.25 cm^{-1} is shifted to 2851.06 cm^{-1} , the amide C=O stretching at 1637.78 cm^{-1} is shifted to

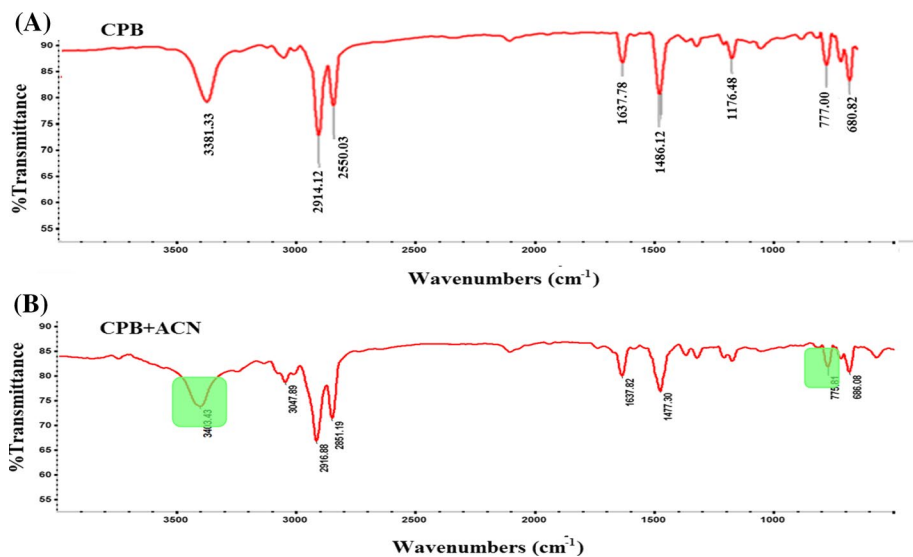


Fig. 8 DRS-FTIR spectra of **a** pure CPB and **b** CPB-ACN

1640.02 cm^{-1} , the C-H bending aromatic C=C stretching vibration at 1471.48 cm^{-1} is shifted to 1484.03 cm^{-1} , and the *cis*=C-H out-of-plane bending at 783.29 cm^{-1} is shifted to 777.85 cm^{-1} . The absorption peaks of CPB are shown in (Fig. 8), the O-H stretching at 3381.33 cm^{-1} is shifted to 3403.43 cm^{-1} , the asymmetric CH_2 , symmetric CH_3 , CH_2 stretching vibration 2914.12 cm^{-1} is shifted to 2916.88 cm^{-1} , the alkyl C-H stretch at 2850.03 cm^{-1} is shifted to 2851.19 cm^{-1} , the amide C=O stretching 1637.78 cm^{-1} is shifted to 1637.82 cm^{-1} , the C-H bending aromatic C=C stretching vibration at 1472.62 cm^{-1} is shifted to 1477.30 cm^{-1} , and the *cis*=C-H out-of-plane bending at 777.00 cm^{-1} is shifted to 775.81 cm^{-1} . The surfactant and ACN interactions vary in the order; TTAB > CTAB > CPC > CPB as is clear from Figs. 5, 6, 7 and 8.

4 Conclusion

In conclusion, the effect of acetonitrile on micellization behavior of four conventional cationic surfactants, viz. CTAB, TTAB, CPC and CPB was studied and analyzed by the conductivity, surface tension and fluorescence methods. In general, the *CMC* values of the four cationic surfactants increase with increasing the V/V% of CAN. It was concluded that the electrostatic and hydrophobic interactions of the solvent with surfactant molecules bring about the dramatic change in the aggregation behavior or micelle formation of all four surfactant systems. The *CMC* and A_{\min} values increase, whereas the Γ_{\max} value decreases with increase in the V/V% of ACN. The negative values of $\Delta G_{\text{M}}^{\circ}$ and $\Delta G_{\text{ads}}^{\circ}$ indicate spontaneous and favorable micellization behavior. The FT-IR qualitative analysis studies confirm the alterations produced within the mixtures of surfactants and organic solvent, which shows that structural variations occurred in the systems. The present study can provide insight into the choice of mixed solvent systems for their use in increased oil recovery, pharmaceutical and cosmetic applications, washings, chemical reactions, etc.

Table 5 Characteristic FT-IR spectra of CTAB, TTAB, CPC and CPB before and after acetonitrile irradiation

Assignment	Characteristic transmittance band (cm ⁻¹)							
	Pure CTAB	CTAB + ACN	Pure TTAB	TTAB + ACN	Pure CPC	CPC + ACN	Pure CPB	CPB + ACN
1 O-H stretching					3371.74	3404.06	3381.33	3403.43
2 Alkenyl C-H stretch	3012.90	3297.18	3010	3015.42			3050	3047.89
3 Asymmetric CH ₂ , symmetric CH ₃ , CH ₂ stretching vibration			2915.72	2917.75	2912.35	2923.13	2914.12	2916.88
4 Alkyl C-H stretch	2849.80	2855.14	2848.49	2849.74	2848.25	2851.06	2850.03	2851.19
5 Amide C=O stretching					1637.78	1640.02	1637.78	1637.82
6 Symmetric and asymmetric stretching C-H scissoring vibration of CH ₃ -N ⁺ moiety	1480, 1435	1459.98			1471.48	1484.03	1472.62	1477.30
7 C-N ⁺ stretching bands	961.80	1097.42			1181	1095	1176.48	1180
8 <i>Trans</i> = C-H out of plane bending			910.99	913.29				
9 <i>Cis</i> = C-H out of plane bending/rocking mode of the methylene chain			718.62	725.55	783.29	777.85	777.00	775.81

Acknowledgements The authors are grateful acknowledgement to Prof. Kallol K Ghosh for providing the surface tension and fluorescence instruments and Mrs. Beta Rani Kharko, School of Studies in Chemistry, PT. Ravishankar Shukla University, Raipur (C.G.) for analysis of samples by FTIR spectroscopy.

References

1. Morsy, S.M.I.: Role of surfactants in nanotechnology and their applications. *Int. J. Curr. Microbiol. Appl. Sci.* **3**, 237–260 (2014)
2. Obeid, A.M., Elburi, A., Young, C.L., Mullen, B.A., Tate, J.R., Ferro, A.V.: Formulation of nonionic surfactant vesicles (NISV) prepared by microfluidics for therapeutic delivery of sirna into cancer cells. *Mol. Pharm.* **14**, 2450–2458 (2017)
3. Verma, G., Hassan, P.A.: Self assembled materials: design strategies and drug delivery perspective. *Phys. Chem. Chem. Phys.* **15**, 17016–17028 (2013)
4. Menger, M.F., Galloway, L.A., Chlebowski, E.M.: Surface tension of aqueous amphiphiles. *Langmuir* **21**, 9010–9012 (2005)
5. Azarmi, R., Ashjarian, A.: Type and application of some common surfactants. *J. Chem. Pharm. Res.* **7**, 632–640 (2015)
6. Parris, G.E., Brinckman, F.E.: Reactions which relate to the environmental mobility of arsenic and antimony. I. Quaternization of trimethylarsine and trimethylstibine. *J. Org. Chem.* **40**, 3801–3803 (1975)
7. Kamal, M.S., Hussein, I.A., Sultan, A.S.: Review on surfactant flooding: phase behavior, retention IFT and field applications. *Energy Fuels* **31**, 7701–7720 (2017)
8. Barni, E., Savarino, P., Viscardi, G.: Dye-surfactant interactions and their applications. *Acc. Chem. Res.* **24**, 98–103 (1991)
9. Kandadai, M.A., Mohan, P., Lin, G., Butterfield, A., Skliar, M., Magda, J.J.: Comparison of surfactants used to prepare aqueous perfluoropentane emulsions for pharmaceutical applications. *Langmuir* **26**, 4655–4660 (2010)
10. Lunkenheimer, K., Lind, A., Jost, M.: Surface tension of surfactant solutions. *J. Phys. Chem. B* **107**, 7527–7531 (2003)
11. Das, S., Mondal, S., Ghosh, S.: Physicochemical studies on the micellization of cationic, anionic, and nonionic surfactants in water–polar organic solvent mixtures. *J. Chem. Eng. Data* **58**, 2586–2595 (2013)
12. Vishnyakov, A., Lee, M.T., Neimark, A.V.: Prediction of the critical micelle concentration of nonionic surfactants by dissipative particle dynamics simulations. *J. Phys. Chem. Lett.* **4**, 797–802 (2013)
13. Jusufi, A., Bard, D.N.L., Levine, B.G., Klein, M.L.: Surfactant concentration effects on micellar properties. *J. Phys. Chem. B* **116**, 987–991 (2012)
14. Maeda, H., Muroi, S., Kakehashi, R.: Effects of ionic strength on the critical micelle concentration and the surface excess of dodecyltrimethylamine oxide. *J. Phys. Chem. B* **101**, 7378–7382 (1997)
15. Qazi, M.J., Liefferink, R.W., Schlegel, S.J., Backus, E.H.G., Bonn, D., Shahidzadeh, N.: Influence of surfactants on sodium chloride crystallization in confinement. *Langmuir* **33**, 4260–4268 (2017)
16. Schick, M.J.: Effect of electrolyte and urea on micelle formation. *J. Phys. Chem.* **68**, 3585–3592 (1964)
17. Tadmor, R., Zapata, E.H., Chen, N., Pincus, P., Israelachvili, J.N.: Debye length and double-layer forces in polyelectrolyte solutions. *Macromolecules* **35**, 2380–2388 (2002)
18. Ricceri, R., Romeu, N.V., Taddei, G.: van der Waals interactions in non ionic micelles. *Langmuir* **12**, 913–915 (1996)
19. Dominguez, A., Fernandez, A., Gonzalez, N., Iglesias, E., Montenegro, L.: Determination of critical micelle concentration of some surfactants by three techniques. *J. Chem. Educ.* **74**, 1227–1231 (1997)
20. Fernandez, A.S., Hammond, O.S., Jackson, A.J., Arnold, T., Douth, J., Edler, K.J.: Surfactant–solvent interaction effects on the micellization of cationic surfactants in a carboxylic acid-based deep eutectic solvent. *Langmuir* **33**, 14304–14314 (2017)
21. Rodríguez, A., Graciani, M.D.M., Angulo, M., Moyá, M.L.: Effects of organic solvent addition on the aggregation and micellar growth of cationic dimeric surfactant 12-3-12, 2Br⁻. *Langmuir* **23**, 11496–11505 (2007)
22. Michor, E.L., Berg, J.C.: Temperature effects on micelle formation and particle charging with span surfactants in apolar media. *Langmuir* **31**, 9602–9607 (2015)
23. Sinha, S., Tikariha, D., Lakra, J., Tiwari, A.K., Saha, S.K., Ghosh, K.K.: Effect of polar organic solvents on self-aggregation of some, cationic monomeric and dimeric surfactants. *J. Surfactant Deterg.* **18**, 629–640 (2015)

24. Din, K.U., Koya, P.A.: Effects of solvent media and temperature on the self-aggregation of cationic dimeric surfactant 14-6-14, 2Br^- studied by conductometric and fluorescence techniques. *Langmuir* **26**, 7905–7914 (2010)
25. Bakshi, M.S.: Micelle formation by anionic and cationic surfactants in binary aqueous solvents. *J. Chem. Soc. Faraday Trans.* **89**, 4323–4326 (1993)
26. Sowmiya, M., Tiwari, A.K., Saha, S.K.: Fluorescent probe studies of micropolarity, premicellar and micellar aggregation of non-ionic Brij surfactants. *J. Colloid Interface Sci.* **344**, 97–104 (2010)
27. Akba, H., Kartal, C.: Conductometric studies of hexadecyltrimethylammonium bromide in aqueous solution of ethanol and ethylene glycol. *Colloid J* **68**, 125–130 (2006)
28. Sood, A.K., Sharma, S.: Influence of organic solvents and temperature on the micellization of conventional and gemini surfactants: a conductometric study. *Phys. Chem. Liq.* **54**, 1–16 (2016)
29. Manet, S., Karpichev, Y., Bassani, D., Ahmad, R.K., Oda, R.: Counter anion effect on micellization of cationic gemini surfactants 14-2-14: Hofmeister and other counterions. *Langmuir* **26**, 10645–10656 (2010)
30. Banjare, M.K., Behera, K., Kurrey, R., Banjare, R.K., Satnami, M.L., Pandey, S., Ghosh, K.K.: Self-aggregation of bio-surfactants within ionic liquid 1-ethyl-3-methyl-imidazolium bromide: a comparative study and potential application in antidepressants drug aggregation. *Spectrochim. Acta A* **199**, 376–386 (2018)
31. Banjare, M.K., Kurrey, R., Yadav, T., Sinha, S., Satnami, M.L., Ghosh, K.K.: A comparative study on the effect of imidazolium-based ionic liquid on self-aggregation of cationic, anionic and nonionic surfactants studied by surface tension, conductivity, fluorescence and FTIR spectroscopy. *J. Mol. Liq.* **241**, 622–632 (2017)
32. Pal, A., Pillania, A.: Modulations in surface and aggregation properties of non-ionic surfactant Triton X-45 on addition of ionic liquids in aqueous media. *J. Mol. Liq.* **233**, 243–250 (2017)
33. Islam, M.M., Rahman, M.R., Islam, M.N.: Micellization behavior and thermodynamic properties of *n*-alkyl trimethylammonium bromide surfactants in aqueous media at different temperatures. *Int. J. Sci. Eng. Res.* **6**, 1508–1516 (2015)
34. Israelachvili, J.N.: *Intermolecular and Surface Force*, 2nd edn, pp. 370–378. Academic Press, London (1991)
35. Ko, J.J.S., Oh, S.W., Kim, Y.S., Nakashima, N., Nagadome, S., Sugihara, G.: Adsorption and micelle formation of mixed surfactant systems in water. IV. Three combination of SDS with MEGA-8, -9 and -10. *J. Oleo Sci.* **53**, 109–126 (2004)
36. Banjare, M.K., Behera, K., Satnami, M.L., Pandey, S., Ghosh, K.K.: Self-assembly of a short-chain ionic liquid within deep eutectic solvents. *RSC Adv.* **8**, 7969–7979 (2018)
37. Chen, W., Zuckerman, N.B., Konopelski, J.P., Chen, S.: Pyrene-functionalized ruthenium nanoparticles as effective chemosensors for nitroaromatic derivatives. *Anal. Chem.* **82**, 461–465 (2010)
38. Piotrowicz, E.K., Dziewulska, K., Stangret, J.: An effective method for studying intermolecular interactions in binary liquids with hydrogen bonds; FTIR spectra and *Ab initio* calculations in the *n*-methylformamide-methanol system. *J. Phys. Chem. B* **114**, 5810–5818 (2010)
39. Miller, F.A., Wilkins, C.H.: Infrared spectra and characteristic frequencies of inorganic ions. *Anal. Chem.* **24**, 1253–1294 (1952)

Publisher's Note Springer Nature remains neutral with regard to jurisdictional claims in published maps and institutional affiliations.